

See discussions, stats, and author profiles for this publication at: <https://www.researchgate.net/publication/221681140>

Expression Profiling of Starchy Endosperm Metabolic Proteins at 21 Stages of Wheat Grain Development

ARTICLE in JOURNAL OF PROTEOME RESEARCH · MARCH 2012

Impact Factor: 4.25 · DOI: 10.1021/pr201110d · Source: PubMed

CITATIONS

12

READS

51

4 AUTHORS, INCLUDING:



Ayesha Tasleem-Tahir

5 PUBLICATIONS 38 CITATIONS

[SEE PROFILE](#)



Isabelle Nadaud

French National Institute for Agricultural Rese...

15 PUBLICATIONS 285 CITATIONS

[SEE PROFILE](#)



Gérard Branlard

French National Institute for Agricultural Rese...

131 PUBLICATIONS 2,930 CITATIONS

[SEE PROFILE](#)

Expression Profiling of Starchy Endosperm Metabolic Proteins at 21 Stages of Wheat Grain Development

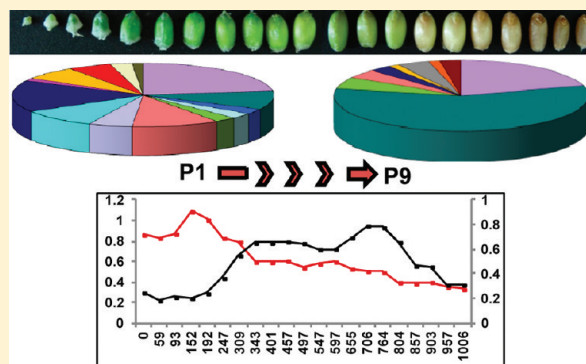
Ayesha Tasleem-Tahir,[†] Isabelle Nadaud,[†] Christophe Chambon,[‡] and Gérard Branlard*,[†]

[†]INRA, UMR 1095 GDEC-UBP, 234 avenue du Brézet, F-63100 Clermont-Ferrand, France

[‡]INRA, QPA, Proteomic Plateforme, F-63122 Saint-Genès Champanelle, France

Supporting Information

ABSTRACT: Proteomic analysis of albumins and globulins (alg) present in starchy endosperm of wheat (*Triticum aestivum* cv Récital), at 21 stages of grain development, led to the identification of 487 proteins. Four main developmental phases of these metabolic proteins, with three subphases in phase three and two in phase four, were shown. Hierarchical cluster analysis revealed nine major expression profiles throughout grain development. Classification of identified proteins in 17 different biochemical functions provided a uniform picture of temporal coordination among cellular processes. Proteins involved in cell division, transcription/translation, ATP interconversion, protein synthesis, protein transport, along with amino acid, lipid, carbohydrate and nucleotide metabolisms were highly expressed in early and early mid stages of development. Protein folding, cytoskeleton, and storage proteins peaked during the middle of grain development, while in later stages stress/defense, folic acid metabolism, and protein turn over were the abundant functional categories. Detailed analysis of stress/defense enzymes revealed three different evolutionary profiles. A global map with their predicted subcellular localizations and placement in grain developmental scale was constructed. The present study of complete grain development enriched our knowledge on proteome expression of alg, successively from endosperm cell division and differentiation to programmed cell death.



KEYWORDS: proteomics, grain development, albumins and globulins, subcellular localization, stress/defense, *Triticum aestivum*

INTRODUCTION

Grain quality improvement is the basic objective of wheat breeding, as wheat grains are the most important food source for humans. The major constituents of wheat grain are starch (70–80% dry weight) and proteins (10–15% dry weight). Of total wheat grain proteins, 80% are prolamins, monomeric gliadins and polymeric glutenins, while the nonprolamin part, albumins and globulins (alg), accounts for 15–20%.¹ Prolamins are the major storage proteins and are well characterized using whole grain or flour extracts.^{2–5} In contrast to prolamins, alg play important roles in cellular metabolism, development and responses to environment as many of them are enzymes or enzyme inhibitors that influence technological quality.^{6,7} Essential amino acids such as aspartate, threonine, lysine, and tryptophan are more abundant in alg as compared to storage proteins. They have complex genetic control, and their role in grain quality is less well understood compared with prolamins.⁸

Changes in metabolite levels can also be coregulated with seed development. Seed development is genetically programmed and can be regulated and influenced by sugar and nitrogen signals.^{9–11} Analysis of results in a developmental context helps to provide detailed knowledge of mechanisms involved in the maturation of targeted sample (grain/tissue). In recent years, proteomic studies have been made on seeds and

seed tissue development in cereals^{12–14} and noncereals.^{15,16} Attempts have been made to characterize alg proteins. For example, Singh et al. reported 19 alg proteins by Edman sequencing,¹⁷ Wong et al. found several thioredoxin targets,¹⁸ Vensel et al. studied 254 alg proteins at two stages of development, and Gao et al. published 230 alg proteins related to wheat quality.^{19,20}

However, this knowledge is too limited to follow alg and related metabolic changes precisely during whole kernel development. To this aim, we studied developmental events of starchy endosperm (a tissue of grain reserve accumulation for the developing embryo) alg from fertilization to maturity at 21 stages of wheat grain development. To complement the results already published, we focused on a very short temporal interval of grain development, nearly at each 50 °Cd (degree days after pollination). We analyzed quantitative and qualitative (presence/absence of protein spots) variations, and we established accumulation profiles of these nonabundant endosperm proteins. We also described interconnections of different biochemical events between adjacent and nonadjacent stages of

Received: November 7, 2011

Published: March 7, 2012

Table 1. Proteins of Starchy Endosperm during Wheat Grain Development (*Triticum aestivum* cv Récital) Identified by LC–MS/MS and Classified by Their Corresponding Metabolic Pathway and Biochemical Functions^a

Spot ID Profile 1	accession	accession after BlastP	Protein name	Predicted sub-cellular localization
Stress/ defense				
1841*	gi257696322	gi3688398	Ascorbate peroxidase	cyto
1876*	gi28192421		Dehydroascorbate reductase	cyto
2659	gi63021412		Salt tolerant protein	cyto
853*	gi684948		Catalase	perox
2094	gi63021412		Salt tolerant protein	cyto
1945*	gi125663927		Manganese superoxide dismutase	cyto
1700*	gi115446749	Q84VC8	Gamma hydroxybutyrate dehydrogenase-like protein	nucl
2151	gi451193		Wal17	cyto
885a	gi18449343		Putative aldehyde dehydrogenase WIS1	M
1837*	gi145326672		Lactoylglutathione lyase, putative	cyto
Transcription / translation				
1789	gi257738538	gi357122287	Predicted 40S ribosomal protein SA	cyto
1510	gi115449323	P17070	Proliferating cell nuclear antigen	nucl
1456	gi242035869		Hypothetical protein SORBIDRAFT_01g036580	cyto
1838	gi242047528		Hypothetical protein SORBIDRAFT_02g003760	M
Amino acid Metabolism				
1138	gi283806355		Aminotransferase	M
1300	gi40317416		Glutamine synthetase isoform GSr1	cyto
960	gi68655466		Putative S-adenosylhomocysteine hydrolase 2	cyto
1299	gi40317416		Glutamine synthetase isoform GSr1	cyto
1315	gi257676137	gi68655495	Methionine synthase 1 enzyme	cyto
1030	gi296514140	gi195622500	Serine hydroxymethyltransferase	cyto
606	gi257676137	gi68655495	Methionine synthase 1 enzyme	cyto
623	gi257676137	gi68655495	Methionine synthase 1 enzyme	cyto
627	gi257676183	gi68655500	Methionine synthase 2 enzyme	cyto
628	gi257676183	gi68655500	Methionine synthase 2 enzyme	cyto
689	gi257635198	gi195649503	Phenylalanine ammonia-lyase	cyto
1234	gi195957723		Aspartate aminotransferase	cyto
Protein turn over				
1686	gi242081935	C5YH32	Proteasome subunit alpha type	cyto
1889	gi52548242		20S proteasome beta 7 subunit	cyto
1844	gi195611928		Proteasome subunit beta type 1	cyto
1925	gi52548238		20S proteasome beta 4 subunit	cyto
1833	gi115447473	Q6H852	Proteasome subunit alpha type	cyto
1805	gi117670154	gi50080305	Putative proteasome subunit alpha type 3	cyto
Protein synthesis				
744	gi226533868		Heat shock protein 70	M
1778	gi108706531		40S ribosomal protein SA, putative, expressed	cyto
1816	gi108706531		40S ribosomal protein SA, putative, expressed	cyto
701	gi2827002		HSP70	cyto
739	gi226533868		Heat shock protein 70	M
713	gi188011548		Heat shock protein 70	cyto
700	gi115486793	gi21664287	Heat shock protein 70	cyto
Protein Folding				
1484	gi47118046		Protein disulfide isomerase	ER
1654	gi1729864		T-complex protein 1 subunit epsilon	cyto
2142	gi13925737		Cyclophilin A-3	cyto
986	gi296524608	gi56606827	Calreticulin-like protein	ER
Carbohydrate metabolism				
798*	gi158701881		NADP-dependent malic enzyme	cyto
994*	gi291047856	gi20530127	Mitochondrial aldehyde dehydrogenase	M
615	gi227483057	gi28190676	Putative transketolase	P
892	gi296523708	gi162457852	Pyruvate decarboxylase isozyme 3	cyto
604	gi227483057	gi28190676	Putative transketolase	P
1113*	gi218401053	gi108708038	Fumarate hydratase 1	M
1908	gi122171022		Soluble inorganic pyrophosphatase	Cysk
1305	gi28172909		Cytosolic 3-phosphoglycerate kinase	cyto
735	gi18076790		Phosphoglucomutase	cyto
1310	gi2204226		Alpha-galactosidase	nucl
1183	gi242064362		Hypothetical protein SORBIDRAFT_04g006440	M
885b*	gi218196143	B8AYE1	Dihydrolipoamide dehydrogenase	M
1033	gi6136111		UTP–glucose-1-phosphate uridylyltransferase	cyto
1855	gi259703023	gi11124572	Triosephosphat-isomerase	cyto

Table 1. continued

Spot ID	accession	accession after BlastP	Protein name	Predicted sub- cellular localization
1483	gi226316439		Fructose-bisphosphate aldolase	cyto
1436*	gi115465579	Q6F361	Malate dehydrogenase	M
1419	gi223018643		Fructose-bisphosphate aldolase	P
1418	gi223018643		Fructose-bisphosphate aldolase	P
1012	gi6136111		UTP-glucose-1-phosphate uridylyltransferase	cyto
1455*	gi195628708		Malate dehydrogenase	M
877	gi18449343		Putative aldehyde dehydrogenase WIS1	M
1444*	gi115465579	Q6F361	Malate dehydrogenase	M
2635	gi18181983		Myo-inositol-1-phosphate synthase	cyto
1200	gi288814543		Alpha amylase	Extr
778	gi32400802		Phosphoglycerate mutase	cyto
1489*	gi32400786		NADPH-dependent mannose 6-phosphate reductase	perox
1427	gi32400859		Aldolase	P
1413	gi32400859		Aldolase	P
2126	gi259703023	gi11124572	Triosephosphat-isomerase	cyto
775	gi32400802		Phosphoglycerate mutase	cyto
1020*	gi242089615	C5Z0L0	Dihydrolipoyl dehydrogenase	P
Cell Wall				
1319	gi50659026		UDP-D-glucuronate decarboxylase	P
ATP Interconversion				
978	gi227303166	gi525291	ATP synthase beta subunit	M
1441*	gi20302473		Ferredoxin-NADP(H) oxidoreductase	P
Cell division				
390	gi257716429	gi357114006	Predicted cell division control protein 48 homolog E-like	cyto
Protein Transport				
1847*	gi126583387		Ferritin	P
Lipid Metabolism				
1532*	gi115478314		Os09g0277800	P
1479*	gi115475922		Os08g0327400	P
1723*	gi296510409	gi195626012	NADH-cytochrome b5 reductase-like protein	M
Nucleotide metabolism				
1323	gi4582787		Adenosine kinase	cyto
1321	gi4582787		Adenosine kinase	cyto
Unknown protein function				
1456a	gi115452789		Os03g0327600	cyto
2180	gi132270		Rubber elongation factor protein	cyto
Profile 2				
Stress/ defense				
1811*	gi15808779		Ascorbate peroxidase	cyto
1007*	gi238802280		Putative Td650 protein	cyto
1782*	gi15808779		Ascorbate peroxidase	cyto
1013*	gi238802280		Putative Td650 protein	cyto
1195	gi296511991	gi4666287	Cytosolic monodehydroascorbate reductase	cyto
1000	gi238802280		Putative Td650 protein	cyto
583	gi556673		Heat shock protein	P
1281	gi242038719		Hypothetical protein SORBIDRAFT_01g013540	P
Transcription/ translation				
2186	gi226497596	gi195604208	40S ribosomal protein S12	cyto
751	gi222629159		Hypothetical protein OsJ_15377	Extr
1098	gi257726667	gi162458395	Translational initiation factor eIF-4A	cyto
1373	gi242075424	gi18391211	TIF3H1; translation initiation factor	cyto
1110	gi257726665	gi162462542	Translational initiation factor	cyto
1249	gi257738538	gi357122287	Predicted 40S ribosomal protein SA	cyto
Amino acid Metabolism				
213	gi222618703		Hypothetical protein OsJ_02282	P
1275	gi506383		Glutamate 1-semialdehyde aminotransferase	P
612*	gi60686892		Delta 1-pyrroline-5-carboxylate synthetase	cyto
616	gi60686892		Delta 1-pyrroline-5-carboxylate synthetase	cyto
624	gi257676183	gi68655500	Methionine synthase 2 enzyme	cyto
2009	gi259439698	gi40363759	Putative glycine-rich protein	nucl
1473	gi295421187	gi585032	Cysteine synthase	cyto
847	gi109940331	gi28912436	Acetohydroxyacid synthase	cyto
1324bis	gi164471780		Aspartate aminotransferase	cyto
1042	gi115487944	Q2QVC1	Argininosuccinate synthase	P

Table 1. continued

Spot ID	accession	accession after BlastP	Protein name	Predicted sub- cellular localization
Protein turn over				
1216	gi296524722	gi225216858	26S protease regulatory subunit S10B	cyto
1055	gi296525618	gi293331089	26S protease regulatory subunit 6B	cyto
1451	gi259662487	gi357146909	Proteasome subunit alpha type-1-like	cyto
1537	gi115435850	Q9SDD1	26S proteasome regulatory particle non-ATPase subunit11	nucl
Protein synthesis				
1215	gi115473357	Q8H3I3	Putative 40S ribosomal protein	cyto
601	gi254211611		70 kDa heat shock protein	P
654	gi476003		HSP70	ER
602	gi254211611		70 kDa heat shock protein	P
656	gi115477547	Q6ZD35	Putative glycyl-tRNA synthetase	M
1754	gi170753		Initiation factor (iso)4F p28 subunit	cyto
658	gi242033449	C5WQD6	Hypothetical protein SORBIDRAFT_01g012680	M
428	gi4103152		Histidyl-tRNA synthetase	cyto
Protein Folding				
1114	gi299469382		Putative PDI-like protein	ER
1092	gi299469382		Putative PDI-like protein	ER
857	gi115459800	Q7FAT6	T-complex protein 1 subunit alpha	cyto
772	gi296087296	gi15232923	Putative chaperonin	cyto
Carbohydrate metabolism				
1067	gi1707930		Glucose-1-phosphate adenylyltransferase large subunit	P
1578	gi46805452		Putative inorganic pyrophosphatase	P
1077	gi148508784		Glyceraldehyde-3-phosphate dehydrogenase	M
370	gi222628767		Hypothetical protein OsJ_14584	M
1294	gi115447367	Q6K9N6	Succinyl-CoA synthetase beta chain	M
1370	gi125560179	A2YRB6	Transaldolase family protein	P
1106	gi224021585		Plastid ADP-glucose pyrophosphorylase small subunit	P
			Dihydrolipoylysine-residue succinyltransferase component of 2-oxoglutarate dehydrogenase complex	M
1072	gi226532024		Pyrophosphate--fructose-6-phosphate 1-phototransferase	P
824	gi115467370	gi15221156	Glucose-1-phosphate adenylyltransferase large subunit	P
1044	gi1707930			
810	gi115448277	Q6ZFT9	Putative diphosphate-fructose-6-phosphate 1-phototransferase alpha chain	cyto
1116	gi218401053	gi108708038	Fumarate hydratase 1	M
1324	gi298541521	gi129916	Phosphoglycerate kinase, cytosolic	cyto
779	gi162957175		NADP-dependent malic enzyme 1	P
823	gi115467370	gi15221156	Pyrophosphate--fructose-6-phosphate 1-phototransferase	P
848	gi115467370	gi15221156	Pyrophosphate--fructose-6-phosphate 1-phototransferase	P
2664*	gi229358240		Cytosolic malate dehydrogenase	cyto
803	gi259708196	F2CX32	Pyruvate kinase	cyto
Signal transduction				
1694	gi227473229	gi112684	14-3-3-like protein	cyto
1410	gi126517972		Serine/threonine-protein phosphatase PP2A-1 catalytic subunit	cyto
Cell wall				
1364	gi4158230		Amylogenin	cyto
ATP Interconversion				
1061	gi296525622		Os06g0192600	Cysk
899	gi81176509		ATP1	M
325	gi222612529		Hypothetical protein OsJ_30891	cyto
283	gi222623539		Hypothetical protein OsJ_08115	ER
Cell division				
1608b	gi257666590	gi149392635	Nucleosome chromatin assembly protein	cyto
415	gi257716429	gi357114006	Predicted cell division control protein 48 homolog E-like	cyto
Protein Transport				
1766	gi16903082		Small Ras-related GTP-binding protein	cyto
1608a	gi297829788	gi15230476	Nascent polypeptide-associated complex subunit alpha-like protein 1	cyto
1740	gi195623482		Coatomer subunit epsilon	cyto
290	gi34393573		Putative karyopherin-beta 3 variant	cyto
Lipid Metabolism				
1494	gi242036027		Hypothetical protein SORBIDRAFT_01g038160	M
Cytoskeleton				
1196	gi58533119		Actin	Cysk
1207	gi226858185		Actin	Cysk
Profile 3				
Stress/ defense				
2544	gi2130114		Trypsin inhibitor CMx precursor	ER

Table 1. continued

Spot ID	accession	accession after BlastP	Protein name	Predicted sub-cellular localization
1907*	gi259017810		Dehydroascorbate reductase	cyto
1685*	gi257696322	gi3688398	Ascorbate peroxidase	cyto
2293	gi134034577		Monomeric alpha-amylase inhibitor	Extr
Transcription/translation				
391	gi115462779	Q6F353	Putative minichromosome maintenance family protein	nucl
2340	gi114145394		Glycine-rich RNA-binding protein	nucl
Amino acid Metabolism				
2636	gi68655466		Putative S-adenosylhomocysteine hydrolase 2	cyto
799	gi242091437	gi195627844	Ketol-acid reductoisomerase	P
Protein turn over				
1806	gi212721808	B4FDY6	Proteasome subunit alpha type	cyto
1964	gi242064246	C5XWW6	Proteasome subunit beta type	nucl
1673	gi242081935	C5YH32	Proteasome subunit alpha type	cyto
1915	gi49388033		Proteasome subunit beta type 3	cyto
Carbohydrate metabolism				
1543	gi7579064		Cytosolic glyceraldehyde-3-phosphate dehydrogenase	cyto
1235	gi298549023	gi226499486	Isocitrate dehydrogenase2	cyto
1124	gi226506764	B4FRC9	Transaldolase 2	P
408	gi75225211		Putative aconitate hydratase	cyto
959	gi195619804		Enolase	cyto
936	gi195619804		Enolase	cyto
1352*	gi229358240		Cytosolic malate dehydrogenase	cyto
1286	gi115447367	Q6K9N6	Succinyl-CoA synthetase beta chain	M
1374*	gi229358240		Cytosolic malate dehydrogenase	cyto
2549	gi210063883		Putative glucose-1-phosphate adenylyltransferase large subunit 1	P
943	gi115455455	gi195623986	UDP-glucose 6-dehydrogenase	ER
ATP Interconversion				
2283b	gi56784991		Putative ATP synthase beta subunit	M
1262	gi108925853		Vacuolar proton-ATPase C subunit	cyto
984	gi227303166	gi525291	ATP synthase beta subunit	M
2285	gi9652119		Nucleoside diphosphate kinase	cyto
2001	gi242043846	gi226507194	ATP synthase D chain, mitochondrial	M
Cell division				
1011	gi1556446		Alpha tubulin	cyto
1010	gi4098272		Alpha tubulin	cyto
1022	gi1556446		Alpha tubulin	cyto
Protein Transport				
1916	gi165973134	Q5XUV1	ADP-ribosylation factor	M
Lipid Metabolism				
1499	gi242036027		Hypothetical protein SORBIDRAFT_01g038160	M
1339	gi257342281	gi75247720	Stearoyl-ACP desaturase	P
Unknown protein function				
1378	gi226492599		Hypothetical protein LOC100277067	cyto
1845	gi132270		Rubber elongation factor protein	cyto
Profile 4				
Stress/ defense				
1794*	gi15808779		Ascorbate peroxidase	cyto
995*	gi684946		Catalase	perox
2264	gi39578552		Alpha amylase inhibitor CM3	Extr
1865*	gi15808779		Ascorbate peroxidase	cyto
1675*	gi15808779		Ascorbate peroxidase	cyto
1868	gi90959771		Multidomain cystatin	ER
413	gi296529766	gi110623251	Heat shock protein 101	cyto
1784bis	gi283480515		Tri a Bd 27K	Extr
Transcription/translation				
695a	gi115475838		Os08g0314800	cyto
695b	gi242065238	gi32492578	RNA binding protein	nucl
Amino acid Metabolism				
1035	gi1703227		Alanine aminotransferase 2	cyto
441	gi218401616	gi226502106	Glutamyl-tRNA synthetase	cyto
880*	gi242091437	gi195627844	Ketol-acid reductoisomerase	P
611	gi257676137	gi68655495	Methionine synthase 1 enzyme	cyto

Table 1. continued

Spot ID	accession	accession after BlastP	Protein name	Predicted sub- cellular localization
Protein turn over				
1208	gi296524722	gi225216858	26S protease regulatory subunit S10B	cyto
667	gi115450022	Q6K9T1	Oligopeptidase A-like	P
1059	gi115466876	gi6652878	26S proteasome AAA-ATPase subunit RPT1a	cyto
Protein synthesis				
680	gi476003		HSP70	ER
720	gi2827002		HSP70	cyto
653	gi476003		HSP70	ER
666	gi476003		HSP70	ER
Protein Folding				
1860	gi42493199		Cyclophilin A	cyto
980	gi77554944		Bifunctional aminoacyl-tRNA synthetase, putative	cyto
916	gi296524604	Q7Y140	Calreticulin	ER
930	gi296524604	Q7Y140	Calreticulin	ER
Carbohydrate metabolism				
401	gi75225211		Putative aconitate hydratase	cyto
890	gi91694277		Glucose-6-phosphate isomerase	cyto
966	gi1707923		Glucose-1-phosphate adenylyltransferase large subunit 1	P
2657*	gi229358240		Cytosolic malate dehydrogenase	cyto
1376*	gi229358240		Cytosolic malate dehydrogenase	cyto
828	gi115467370	gi15221156	Pyrophosphate-fructose-6-phosphate 1-phosphotransferase	P
998	gi20127139		Small subunit ADP glucose pyrophosphorylase	P
956	gi1707923		Glucose-1-phosphate adenylyltransferase large subunit 1	P
1784	gi257355184	O48556	Soluble inorganic pyrophosphatase	cyto
411	gi92429669		Putative aconitate hydratase 1	P
Cell wall				
1303	gi50659026		UDP-D-glucuronate decarboxylase	P
Lipid Metabolism				
1480	gi242036027		Hypothetical protein SORBIDRAFT_01g038160	M
Profile 5				
Stress/ defense				
2291	gi253783731		Alpha amylase inhibitor CM1	Extr
1255c*	gi119388709		Alcohol dehydrogenase ADH1	cyto
584	gi32765549		Cytosolic heat shock protein 90	cyto
1201	gi75313847		Serpin-Z2A	P
412	gi544242		Glucose-regulated protein 94 homolog	ER
1008*	gi238802280		Putative Td650 protein	cyto
901*	gi291047792	gi300087069	Aldehyde dehydrogenase 7b	perox
Transcription/translation				
1714	gi232033		Elongation factor 1-beta	cyto
1718	gi232033		Elongation factor 1-beta	cyto
2644	gi32400796		Acidic ribosomal protein	M
1095a	gi170776		Translation elongation factor 1 alpha-subunit	cyto
1095b	gi170776		Translation elongation factor 1 alpha-subunit	cyto
1103	gi257726667	gi162458395	Translational initiation factor eIF-4A	cyto
1956	gi257714428	gi195637912	Transcription factor BTF3	nucl
337	gi242065238	gi32492578	RNA binding protein	nucl
1934*	gi75246527		Translationally-controlled tumor protein homolog	cyto
409	gi115446385	Q6H4L2	Elongation factor 2	cyto
788	gi1737492		Poly(A)-binding protein	cyto
1081	gi170776		Translation elongation factor 1 alpha-subunit	cyto
1255a	gi170776		Translation elongation factor 1 alpha-subunit	cyto
Amino acid Metabolism				
212	gi222618703		Hypothetical protein OsJ_02282	P
1028	gi1703227		Alanine aminotransferase 2	cyto
1163	gi194268461		Chorismate synthase	P
1168	gi194268461		Chorismate synthase	P
888	gi242091437	gi195627844	Ketol-acid reductoisomerase	P
922	gi296514168	gi108862549	Serine hydroxymethyltransferase	cyto
442	gi218401616	gi226502106	Glutaminyl-tRNA synthetase	cyto
932	gi296514168	gi108862549	Serine hydroxymethyltransferase	cyto
1043	gi1703227		Alanine aminotransferase 2	cyto
2031	gi259439698	gi40363759	Putative glycine-rich protein	nucl

Table 1. continued

Spot ID	accession	accession after BlastP	Protein name	Predicted sub- cellular localization
Protein synthesis				
585	gi4204859		Heat shock protein 80	cyto
710	gi476003		HSP70	ER
Protein Folding				
907	gi6671939		Putative T-complex protein 1, ETA subunit	cyto
834	gi47118046		Protein disulfide isomerase	ER
1301	gi299469378		Putative PDI-like protein	ER
2634	gi242032147		Hypothetical protein SORBIDRAFT_01g000380	P
2145a	gi13925737		Cyclophilin A-3	cyto
2145b	gi42493199		Cyclophilin A	cyto
Carbohydrate metabolism				
967	gi1707930		Glucose-1-phosphate adenylyltransferase large subunit	P
1798	gi259662377	gi226529672	Triosephosphate isomerase, cytosolic	cyto
1255b	gi298549023	gi226499486	Isocitrate dehydrogenase2	cyto
769	gi32400802		Phosphoglycerate mutase	cyto
568	gi401138		Sucrose synthase 1	M
540	gi11037530		Starch branching enzyme 1	P
2650	gi148508784		Glyceraldehyde-3-phosphate dehydrogenase	M
569	gi401138		Sucrose synthase 1	M
1202*	gi242095836	gi195640660	Formate dehydrogenase 1	M
348	gi183211902		Plastid alpha-1,4-glucan phosphorylase	P
1191*	gi242095836	gi195640660	Formate dehydrogenase 1	M
546	gi11037530		Starch branching enzyme 1	P
344	gi183211902		Plastid alpha-1,4-glucan phosphorylase	P
326	gi222628767		Hypothetical protein OsJ_14584	M
1256*	gi242095836	gi195640660	Formate dehydrogenase 1	M
1259*	gi242095836	gi195640660	Formate dehydrogenase 1	M
774	gi115476012	Q84QT9	Putative pyrophosphate-dependent phosphofructokinase alpha subunit	cyto
1004	gi20127139		Small subunit ADP glucose pyrophosphorylase	P
Signal transduction				
1681	gi2492487		14-3-3-like protein B	cyto
1680	gi2492487		14-3-3-like protein B	cyto
1639	gi257664738	gi2266662	14-3-3 protein	cyto
1193	gi297851506		GTP binding protein	cyto
1643	gi257664738	gi2266662	14-3-3 protein	cyto
1644	gi257664738	gi2266662	14-3-3 protein	cyto
1634	gi257664738	gi2266662	14-3-3 protein	cyto
ATP Interconversion				
399	gi254256262	E9NQE5	Pyruvate orthophosphate dikinase 1	P
398	gi254256262	E9NQE5	Pyruvate orthophosphate dikinase 1	P
Cell division				
397	gi257716429	gi357114006	Predicted cell division control protein 48 homolog E-like	cyto
Protein Transport				
757	gi45357045		Coatomer alpha subunit	M
Folic acid metabolism				
717	gi242044850		Hypothetical protein SORBIDRAFT_02g026140	P
715	gi242044850		Hypothetical protein SORBIDRAFT_02g026140	P
730	gi242044850		Hypothetical protein SORBIDRAFT_02g026140	P
Profile 6				
Stress/ defense				
2205	gi115464233	gi195645676	USP family protein	cyto
Transcription/translation				
1954	gi41400293		S-like RNase	Extr
Amino acid Metabolism				
879*	gi291047652	gi21747870	Betaine-aldehyde dehydrogenase	cyto
Protein synthesis				
2162	gi296512518	gi186886530	16.8 kDa heat-shock protein	cyto
2161	gi296512688	gi123545	16.9 kDa class I heat shock protein 1	cyto
2165	gi296512518	gi186886530	16.8 kDa heat-shock protein	cyto
2166	gi296512797	gi195626536	17.4 kDa class I heat shock protein 3	cyto
2187	gi296512793	gi321266547	Heat shock protein 17	cyto
2135	gi296512688	gi123545	16.9 kDa class I heat shock protein 1	cyto
Protein Folding				
973	gi77554944		Bifunctional aminoacyl-tRNA synthetase, putative	cyto

Table 1. continued

Spot ID	accession	accession after BlastP	Protein name	Predicted sub- cellular localization
Carbohydrate metabolism				
384	gi257665965	gi3341490	Phosphoenolpyruvate carboxylase	cyto
876	gi298545815	gi4588609	Granule bound starch synthase precursor	P
400	gi75225211		Putative aconitate hydratase	cyto
1154	gi298541521	gi129916	Phosphoglycerate kinase, cytosolic	cyto
555	gi3393044		Sucrose synthase type 2	cyto
547	gi3393044		Sucrose synthase type 2	cyto
759	gi18076790		Phosphoglucomutase	cyto
552	gi401138		Sucrose synthase 1	M
1863	gi290875537		Putative carbonic anhydrase	P
Profile 7				
Stress/ defense				
1869*	gi34539782		1-Cys-peroxiredoxin	cyto
2339	gi54778521		0.19 dimeric alpha-amylase inhibitor	Extr
1887*	gi28192421		Dehydroascorbate reductase	cyto
1197	gi75313847		Serpin-Z2A	P
1189	gi224589266		Serpin 1	P
1274	gi224589268		Serpin 2	P
937	gi75313847		Serpin-Z2A	P
Transcription/translation				
761	gi222629159		Hypothetical protein OsJ_15377	Extr
760	gi222629159		Hypothetical protein OsJ_15377	Extr
Amino acid Metabolism				
1135	gi283806359		Alanine-glyoxylate aminotransferase	M
1345	gi164471780		Aspartate aminotransferase	cyto
2041	gi259439698	gi40363759	Putative glycine-rich protein	nucl
1435	gi212276289	B4F833	Diaminopimelate epimerase	P
Protein synthesis				
2224	gi75766428		Chain L,Negative Stain Em Reconstruction Of M.Tuberculosis Acr1(Hsp 16.3)	cyto
Protein Folding				
2637	gi242032147		Hypothetical protein SORBIDRAFT_01g000380	P
839	gi13925726		Protein disulfide isomerase 2 precursor	ER
Carbohydrate metabolism				
1472	gi32400764		Beta amylase	Extr
560	gi401138		Sucrose synthase 1	M
539	gi11037530		Starch branching enzyme 1	P
554	gi3393044		Sucrose synthase type 2	cyto
570	gi3393044		Sucrose synthase type 2	cyto
571	gi3393044		Sucrose synthase type 2	cyto
576	gi3393044		Sucrose synthase type 2	cyto
573	gi3393044		Sucrose synthase type 2	cyto
561	gi3393044		Sucrose synthase type 2	cyto
918	gi91694277		Glucose-6-phosphate isomerase	cyto
718a	gi20259685		Beta-D-glucan exohydrolase	ER
1386	gi148508784		Glyceraldehyde-3-phosphate dehydrogenase	M
1318	gi253783729		Glyceraldehyde-3-phosphate dehydrogenase	cyto
1404*	gi125561648	A2YV15	Malate dehydrogenase	P
1372	gi148508784		Glyceraldehyde-3-phosphate dehydrogenase	M
1458	gi34485587		Plastidic alpha 1,4-glucan phosphorylase 3	cyto
1332	gi226316439		Fructose-bisphosphate aldolase	cyto
1399*	gi229358240		Cytosolic malate dehydrogenase	cyto
920	gi91694277		Glucose-6-phosphate isomerase	cyto
2660*	gi229358240		Cytosolic malate dehydrogenase	cyto
2654*	gi229358240		Cytosolic malate dehydrogenase	cyto
Signal transduction				
1554	gi257672913	gi162459667	Annexin p33	cyto
Cell wall				
934	gi6175480		Xylose isomerase	ER
Protein Transport				
1971	gi115447377	Q6K1Q5	Glycolipid transfer protein-like	cyto
Storage Proteins				
1595	gi295853625		Avenin-like b	ER
1742	gi110341795		Globulin 1	ER

Table 1. continued

Spot ID	accession	accession after BlastP	Protein name	Predicted sub-cellular localization
Folic acid metabolism				
1521	gi115589734		5,10-methylene-tetrahydrofolate dehydrogenase	cyto
Unknown protein function				
2553	gi132270		Rubber elongation factor protein	cyto
Profile 8				
Stress/ defense				
1406*	gi257710966	gi62765876	2-alkenal reductase	cyto
1614*	gi159895412		NADPH-dependent thioredoxin reductase isoform 2	cyto
2256	gi221855656		Alpha-amylase inhibitor CM16 subunit	Extr
1190	gi75313847		Serpin-Z2A	P
1351	gi224589270		Serpin 3	P
1330a	gi75279909		Serpin-Z2B	P
1679	gi51247633		Chain A, Crystal Structure Of Family 11 Xylanase In Complex With Inhibitor	Extr
1186	gi75313848		Serpin-Z1C	P
1221	gi75313848		Serpin-Z1C	P
1165	gi224589266		Serpin 1	P
2545	gi55669878		Chain B, Crystal Structure Of The Triticum aestivum Xylanase Inhibitor-I	cyto
1265	gi224589268		Serpin 2	P
1175	gi75313848		Serpin-Z1C	P
1317	gi75313848		Serpin-Z1C	P
1757	gi51247633		Chain A, Crystal Structure Of Family 11 Xylanase In Complex With Inhibitor	Extr
1270	gi224589268		Serpin 2	P
1817	gi62465514		Class II chitinase	ER
2230	gi114215938		Dimeric alpha-amylase inhibitor	Extr
439	gi296529766	gi110623251	Heat shock protein 101	cyto
1615	gi226495167		Desiccation-related protein PCC13-62	ER
1645	gi145326672		Lactoylglutathione lyase, putative	cyto
1687	gi156186245		Xylanase inhibitor 725ACCN	ER
2214*	gi226897529		Superoxide dismutase	cyto
2270*	gi226897529		Superoxide dismutase	cyto
Amino acid Metabolism				
923	gi296514168	gi108862549	Serine hydroxymethyltransferase	cyto
Protein synthesis				
2266	gi75766428		Chain L,Negative Stain Em Reconstruction Of M.Tuberculosis Acr1(Hsp 16.3)	cyto
2206	gi75766428		Chain L,Negative Stain Em Reconstruction Of M.Tuberculosis Acr1(Hsp 16.3)	cyto
1944	gi157093720	gi18397757	Basic secretory protein family protein	ER
1227	gi2827002		HSP70	cyto
Protein Folding				
1589	gi299469378		Putative PDI-like protein	ER
870	gi2493650		60 kDa chaperonin subunit beta	cyto
862	gi2493650		60 kDa chaperonin subunit beta	cyto
Carbohydrate metabolism				
898	gi32400764		Beta amylose	Extr
909	gi38349539		Beta-amylase 1	Extr
1330b	gi298541521	gi129916	Phosphoglycerate kinase, cytosolic	cyto
1356	gi226316439		Fructose-bisphosphate aldolase	cyto
910	gi195619804		Enolase	cyto
1347	gi4158232		Reversibly glycosylated polypeptide	cyto
1366a	gi226316439		Fructose-bisphosphate aldolase	cyto
1366	gi226316439		Fructose-bisphosphate aldolase	cyto
1393*	gi229358240		Cytosolic malate dehydrogenase	cyto
1333	gi3646373		RGP1 protein	cyto
968	gi193073259		Beta-glucosidase	ER
1295	gi253783729		Glyceraldehyde-3-phosphate dehydrogenase	cyto
Signal transduction				
1667	gi227473229	gi112684	14-3-3-ike protein A	cyto
Cell wall				
1767	gi40363753		Putative caffeoyl CoA O-methyltransferase	cyto
1768	gi40363753		Putative caffeoyl CoA O-methyltransferase	cyto
Storage Proteins				
1691	gi133741924		Gamma gliadin	ER
Profile 9				
Stress/ defense				
2395*	gi226897529		Superoxide dismutase	cyto

Table 1. continued

Spot ID	accession	accession after BlastP	Protein name	Predicted sub- cellular localization
1929*	gi257333180	Q8RW03	Glutathione transferase	cyto
1913	gi20257409		Thaumatin-like protein	ER
2350	gi54778521		0.19 dimeric alpha-amylase inhibitor	Extr
2480	gi134034647		Monomeric alpha-amylase inhibitor	Extr
2443	gi1588926		Pathogenesis-related protein	Extr
2350a	gi54778521		0.19 dimeric alpha-amylase inhibitor	Extr
2648	gi39578552		Alpha amylase inhibitor CM3	Extr
2649	gi39578552		Alpha amylase inhibitor CM3	Extr
2442	gi54778511		0.19 dimeric alpha-amylase inhibitor	Extr
2083	gi123975		Endogenous alpha-amylase/subtilisin inhibitor	cyto
2402	gi283465827		Putative alpha-amylase inhibitor CM2	Extr
2328	gi54778521		0.19 dimeric alpha-amylase inhibitor	Extr
2364	gi54778521		0.19 dimeric alpha-amylase inhibitor	Extr
2463	gi134034647		Monomeric alpha-amylase inhibitor	Extr
2423	gi134034647		Monomeric alpha-amylase inhibitor	Extr
1812	gi62465514		Class II chitinase	ER
1890	gi14164981		Thaumatin-like protein	ER
1931	gi20257409		Thaumatin-like protein	ER
1829	gi62465514		Class II chitinase	ER
Chain A ,Crystal Structure Of Family 11 Xylanase In Complex With Inhibitor (XiP-I)				
1769	gi51247633		Aldose reductase	Extr
1504	gi113595		0.19 dimeric alpha-amylase inhibitor	cyto
2421	gi54778511		Monomeric alpha-amylase inhibitor	Extr
2475	gi134034647		Alpha amylase inhibitor CM3	Extr
2309	gi39578552		0.19 dimeric alpha-amylase inhibitor	Extr
2411	gi54778511		Dimeric alpha-amylase inhibitor	Extr
2387	gi114215876		Monomeric alpha-amylase inhibitor	Extr
2420	gi134034647		Dimeric alpha-amylase inhibitor	Extr
2358	gi114215938		Dimeric alpha-amylase inhibitor	Extr
2347	gi65993872		Dimeric alpha-amylase inhibitor	Extr
2333	gi114215938		Dimeric alpha-amylase inhibitor	Extr
1996	gi224589266		Serpin 1	P
1946*	gi125663927		Manganese superoxide dismutase	cyto
1943*	gi125663927		Manganese superoxide dismutase	cyto
1943a*	gi1621627		Manganese superoxide dismutase	M
Chain B, Crystal Structure Of The Triticum aestivum Xylanase Inhibitor-I				
1280	gi55669878		Serpin-Z1C	cyto
1185	gi75313848		Serpin-Z1B	P
1177	gi75279910		Serpin-Z2B	P
1156	gi75279909		Serpin-Z1B	P
1167	gi75279910		Chitinase	ER
1565	gi495305		Dimeric alpha-amylase inhibitor	Extr
2354	gi114215938			
Amino acid Metabolism				
1278*	gi242073884	gi81686712	Glutamate dehydrogenase 2	M
1369	gi164471780		Aspartate aminotransferase	cyto
Protein turn over				
1900	gi66271071		Beta1 proteasome-1D	cyto
2404	gi257708815	P55857	Small ubiquitin-related modifier 1	cyto
2061	gi211906468		20S proteasome subunit alpha-1	cyto
1497	gi259662487	gi357146909	Proteasome subunit alpha type-1-like	cyto
Protein synthesis				
1260	gi2827002		HSP70	cyto
1279	gi476003		HSP70	ER
1213	gi476003		HSP70	ER
Protein Folding				
874	gi222446344		Protein disulfide isomerase	ER
Carbohydrate metabolism				
883	gi38349539		Beta-amylase 1	Extr
883a	gi38349539		Beta-amylase 1	Extr
882	gi38349539		Beta-amylase 1	Extr
837	gi32400764		Beta-amylase	Extr
836	gi32400764		Beta-amylase	Extr
2651	gi148508784		Glyceraldehyde-3-phosphate dehydrogenase	M

Table 1. continued

Spot ID	accession	accession after BlastP	Protein name	Predicted sub-cellular localization
1355	gi226316439		Fructose-bisphosphate aldolase	cyto
1365a	gi226316439		Fructose-bisphosphate aldolase	cyto
974	gi193073259		Beta-glucosidase	ER
965	gi193073259		Beta-glucosidase	ER
975	gi193073259		Beta-glucosidase	ER
1365b	gi226316439		Fructose-bisphosphate aldolase	cyto
1380	gi148508784		Glyceraldehyde-3-phosphate dehydrogenase	M
1415*	gi125561648	A2YVI5	Malate dehydrogenase	P
889	gi38349539		Beta-amylase 1	Extr
Storage Proteins				
2662	gi110341801		Globulin 1	ER
Folic acid metabolism				
782	gi242044850		Hypothetical protein SORBIDRAFT_02g026140	P
855	gi115589734		5,10-methylene-tetrahydrofolate dehydrogenase	cyto
Unknown protein function				
2646	gi132270		Rubber elongation factor protein	cyto
1950	gi132270		Rubber elongation factor protein	cyto
2383	gi132270		Rubber elongation factor protein	cyto

^aSpot IDs with asterix (*) represent proteins of redox homeostasis. Spot ID; spot number; accession, protein reference found in NCBInr by LC–MS/MS; accession after BlastP, protein reference found in NCBInr or Uniprot; Protein name found in NCBInr or Uniprot; Predicted protein sub-cellular localizations found by using WoLF PSORT, Predotar, TargetP, YLoc and WegoLoc.

development, particularly associated with starch synthesis, starchy endosperm cell death, and stress/defense.

MATERIAL AND METHODS

Material Preparation

Triticum aestivum cv Récital was cultivated in normal wheat growing season (November–July) in a green house at INRA, Clermont-Ferrand, France. Plants were grown under natural soil conditions, fertilized (120 kg N-ha^{-1}), watered as usual and were protected against fungi.

Grains from the middle of the ears were tagged at the date of anthesis. Air temperature close to the ears was recorded and varied between 14.8 and 24.2 °C. Daily mean air temperature was calculated, and the sum of mean temperatures was used to follow the developmental stage in thermal time (°Cd). Wheat grains were harvested every 50 °Cd from anthesis (0 °Cd) to maturity (1006 °Cd) and were stored at –80 °C until dissection.

Dissection was carried out under laminar air flow using binocular for grains of 152–1006 °Cd, whereas whole grains were used for 0–93 °Cd, since they were very small and not fully differentiated. We separated starchy endosperm after removing embryo, brush part and peripheral layers, for study of metabolic proteins. For each developmental stage, the dissected endosperm was weighed and ground in liquid nitrogen using pestle and mortar. The resulting powder was stored at –80 °C until analysis.

Extraction of Alg Proteins

Albumins and globulins (alg) were extracted with low concentrated salt solution (Phosphate 10 mM, NaCl 10 mM, pH 7.8), which was supplemented with a cocktail of plant protease inhibitors (Sigma, St Louis, MO, USA), and was mixed continuously at 4 °C for 2 h.²¹ After centrifugation (8000g, 20 min), the soluble proteins were precipitated with acetone at –20 °C. The pellet of extracted alg proteins was then washed several times with acetone before being dried at room temperature. Alg pellets were dissolved in extraction

buffer 4% (w/v) CHAPS, 7 M urea, 2 M thiourea, 70 mM DTT, 1% (v/v) IPG buffer (pH 3–11 NL), and protease inhibitor cocktail, then the protein content was measured using the Bradford method.²² Protein extracts were either directly used for IEF or were stored at –80 °C until electrophoresis.

Two-Dimensional Separation

Three biological extracts with two replicates per extract were used for analysis of each developmental stage. IEF was performed using the IPGPhor II apparatus (GE Healthcare, Uppsala, Sweden) on 24 cm Immobiline dry strips of 3–11 nonlinear pH gradient. Rehydration of strips was performed overnight at room temperature with 460 μL of solution containing 7 M urea, 2 M thiourea, 1% (v/v) IPG buffer (pH 3–11), 4% (w/v) CHAPS, 1.2% (v/v) destreak reagent (GE Healthcare, Uppsala, Sweden) and few grains of bromophenol blue. Protein extracts (300 μg) were cup-loaded on the acidic side of the strip and IEF was carried out by applying a cumulative voltage of 90 kWh. Following IEF, equilibration of strips, SDS-PAGE and gel staining using CBB G250, were performed as described earlier.¹²

Image and Statistical Analysis

G-800 (GE Healthcare, Uppsala, Sweden) scanner was used to obtain gel images that were then analyzed using SameSpots v4.1 (Nonlinear dynamics, Newcastle, UK). Proteins with fold change ≥ 1.8 , *p*-value of ANOVA and with a *q*-value (measure of false positives in data) less than 0.05 were considered significant. Normalized volume values were used for statistical tests. Hierarchical cluster analysis (HCA) was computed using significant spots (950) for protein clustering according to Pearson's distance.

Protein Identification by LC–MS/MS

A total of 580 out of 950 (significantly varied protein spots), were excised from gels. The spots were destained and digested using the method described previously.¹² For LC–MS/MS analysis, peptide mixtures were analyzed by online nanoflow liquid chromatography using the Ultimate 3000 RSLC (Dionex, Voisins le Bretonneux, France) with nanocapillary columns of

15 cm length \times 75 μm i.d. (Acclaim Pep Map RSLC, Dionex). The solvent gradient increased linearly from 4 to 50% ACN in 0.5% formic acid at a flow rate of 300 nL/min for 30 min. The elute was then electrosprayed in a LTQ-VELOS mass spectrometer (Thermo Fisher Scientific, Courtaboeuf, France) through a nanoelectrospray ion source which was operated in a CID top 10 mode (i.e., 1 full scan MS and the 10 major peaks in the full scan were selected for MS/MS). Full-scan survey MS spectra were acquired with 1 microscan (*m/z* 400–1400). Dynamic exclusion was used with 2 repeat counts, 30 s repeat duration and 60 s exclusion duration. For MS/MS, isolation width for ion precursor was fixed at 3 *m/z*; fragmentation used 35% normalized collision energy at the default activation *q* of 0.25.

Thermo Proteome Discoverer v1.2 was used for raw data file processing. For protein identification, the NCBInr viridiplantae protein database was combined with sequences of human keratin contaminants. The following parameters were considered for the searches: peptide mass tolerance was set to 1.5 Da, fragment mass tolerance was set to 0.8 Da and maximum of two missed cleavages were allowed. Variable modifications were methionine oxidation (M) and carbamidomethylation (C) of cysteine. A protein was considered valid when a minimum of three unique peptides originating from one protein showed statistically significant ($p < 0.01$) Mascot scores (http://www.matrixscience.com/search_form_select.html). For several identification results of one protein spot, we selected the one with highest score for their functional classification (Table 1). Selection was based on the most appropriate taxonomy when Mascot reported alternatives with the same score. High confidence protein identifications in each spot are presented in Table S1 (Supporting Information). During grain development some protein identifications resulted in spots with unknown function. For these proteins, we made a BLASTP in NCBInr or UniProt using the protein sequences identified by LC–MS/MS.²³ The best hits were selected with at least 90% sequence similarity and significant score values.

Proteins were then classified according to KEGG PATHWAY database (<http://www.genome.jp/kegg/pathway.html>) and gene ontology. We established composite expression profiles for each functional category by summing normalized volumes of all the protein spots representative of that category for each developmental stage and then the mean value of 6 replicates was used to draw the expression curves.

Prediction of Subcellular localization

Subcellular localizations of identified proteins were predicted using the following programs: WoLF PSORT,²⁴ Predotar,²⁵ TargetP,²⁶ YLoc²⁷ and WegoLoc.²⁸ Subcellular localizations were added in Table 1, if at least three programs predicted the same localization of a protein at subcellular level.

RESULTS

Wheat endosperm alg proteins were studied at 21 stages during kernel development. Only one gluten protein (gamma-gliadin) was identified, which confirms the effectiveness of the protein separation method. A proteome map of metabolic proteins was developed for the whole kernel development. A total of 1780 spots were detected over the gels, among which 950 were significant on the basis of fold change and *p*- and *q*-values. The proteins above 80 kDa were abundant at early stages while low molecular weight proteins appeared progressively toward grain maturity. There was also a shift of proteins on 2D plane from

acidic to basic zone, with maturity of grain. (Figure S1, Supporting Information)

In PCA results, the first component PC1 and second PC2 explained a total variance of 50.8% (32.5 and 18.3% respectively). Four major phases of development could be differentiated, i.e., (1) 0–93 °Cd; (2) 152–192 °Cd; (3) 247–764 °Cd; (4) 804–1006 °Cd. In addition, three subphases in phase 3 while two in phase 4 were identified (Figure S2, Supporting Information). The same grouping was found by plotting PC1 against PC3 (total variance 38.5%), and PC2 against PC3 (total variance 24.3%). A slight decrease in spot number was observed toward maturity (Figure 1a). The

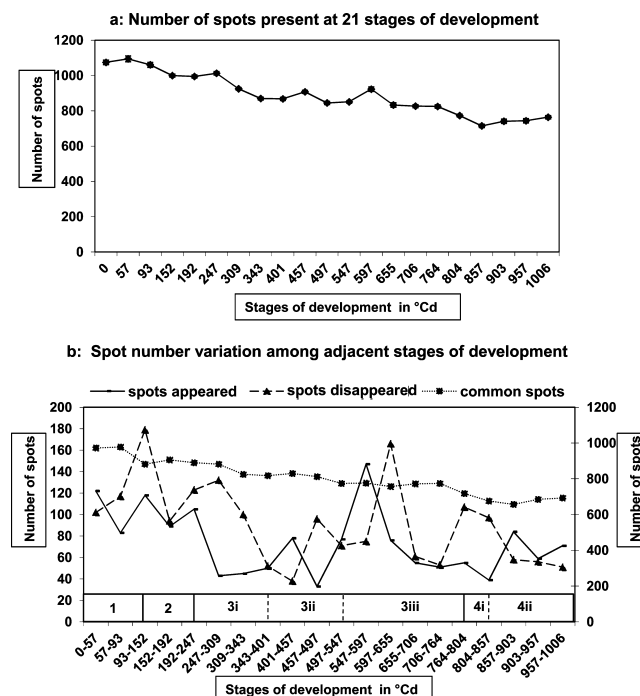


Figure 1. (a) Total spot number present at each stage of development (21 stages). (b) Number of spots that remain common and that appear and disappear between two adjacent stages. Stages of development are on the *x*-axis, while numbers of spots are represented on the *y*-axis.

number of spots that were common and that appeared and disappeared between two adjacent stages are presented in Figure 1b.

Protein Accumulation Clusters

Protein clustering revealed nine expression profiles (P1–P9) using HCA (Figure S3, Supporting Information). Expression tendency of protein spots in corresponding profiles is shown in Figure 2. On the basis of these curves, profiles were grouped in four main clusters as follows:

- Early accumulation cluster (EAC) grouped profiles 1 and 2, P1 with highest accumulation between 0 and 93 °Cd and P2 with a peak at 152 °Cd and then a rapid decrease. These are representative of proteins present in first and second phases of development (Figure S2, Supporting Information).
- Early mid accumulation cluster (EMAC) included profiles 3 and 4, these two profiles peaked at 152 °Cd and 93 °Cd respectively and then decreased with grain maturity. In P3 proteins accumulated again at 903 °Cd

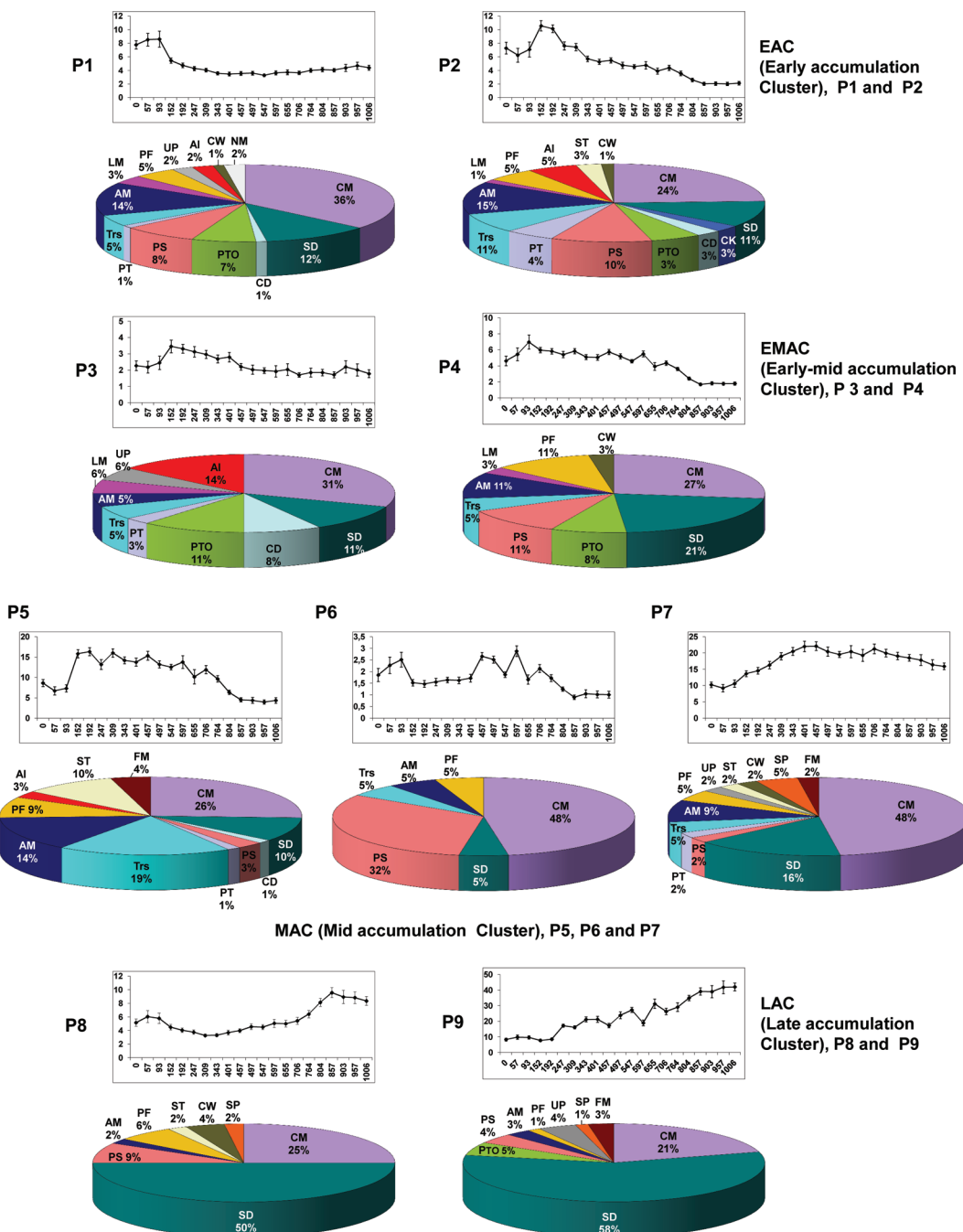


Figure 2. Functional distribution of proteins identified in each of the nine profiles. Each profile evolution is indicated by the curve above the corresponding pie chart, normalized volume is on the vertical axis, and stages of development (in °Cd) are on the horizontal axis with SD bars where $n = 6$. The percentage of identified spots included in each category is indicated. AI, ATP interconversion; AM, amino acid metabolism; CD, cell division; CK, cytoskeleton; CM, carbohydrate metabolism; CW, cell wall related; FM, folic acid metabolism; LM, lipid metabolism; PF, protein folding; PS, protein synthesis; PT, protein transport; PTO, protein turn over; SP, storage proteins; ST, signal transduction; SD, stress/defense proteins; Trs, transcription/translation; UP, unknown proteins.

while in P4 from 804 °Cd their expression decreased significantly.

- (iii) Mid accumulation cluster (MAC) was represented by P5, P6 and P7. In P5, proteins were mainly present between 152 and 706 °Cd while in P7 they accumulated between 401 and 706 °Cd. This cluster represented the proteins present largely during second and third phase of development. In contrast to P5 and P7, in P6 proteins were abundant at first and third phase of development

with comparatively very low expression during second and fourth phase.

- (iv) Late accumulation cluster (LAC) was comprised of P8 and P9. Proteins in P8 were accumulated particularly at later stages with a peak at 857 °Cd. In P9, a gradual increase in expression was observed from 247 °Cd which peaked at 1006 °Cd. Proteins of the fourth developmental phase were accumulated mainly in this cluster.

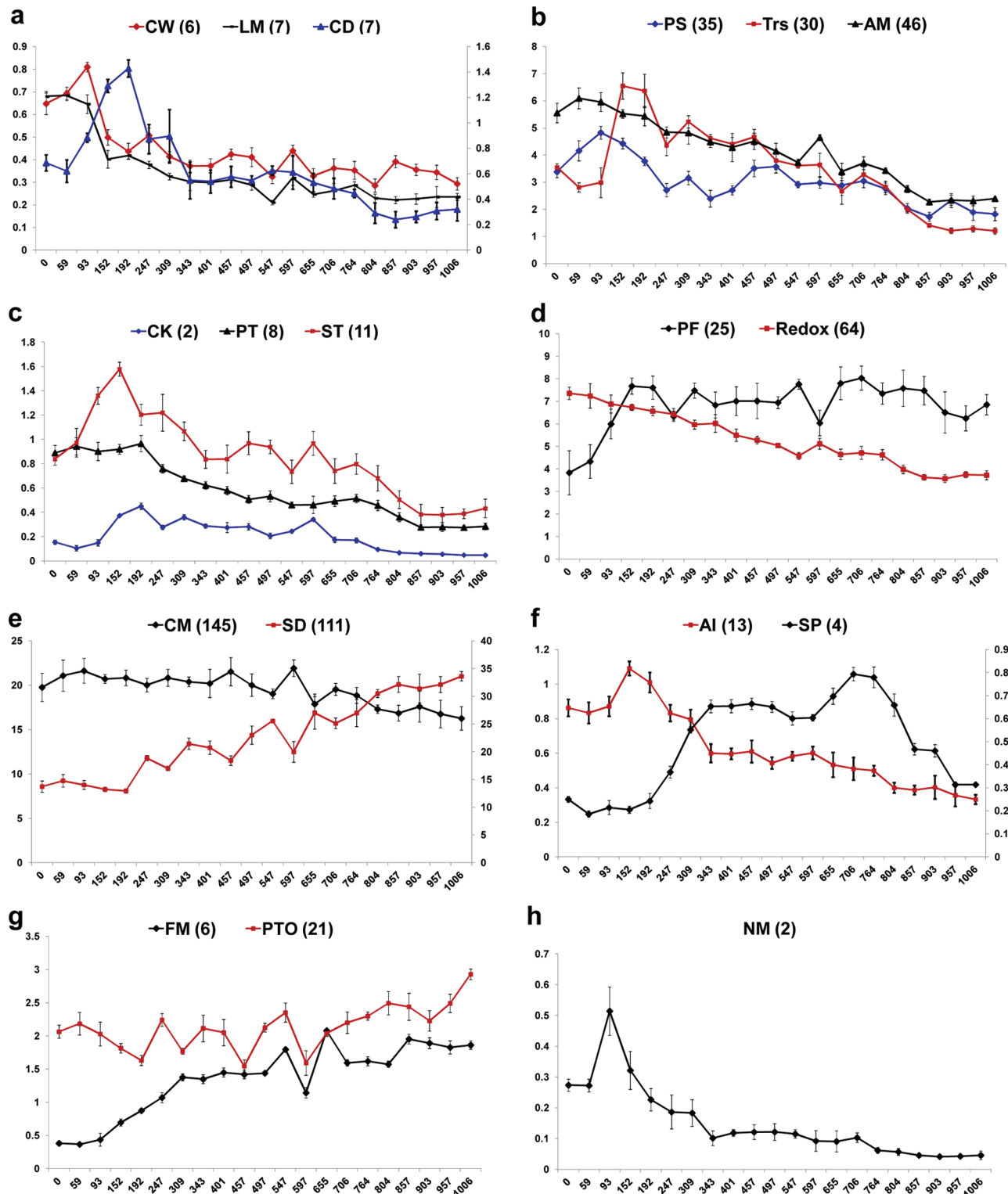
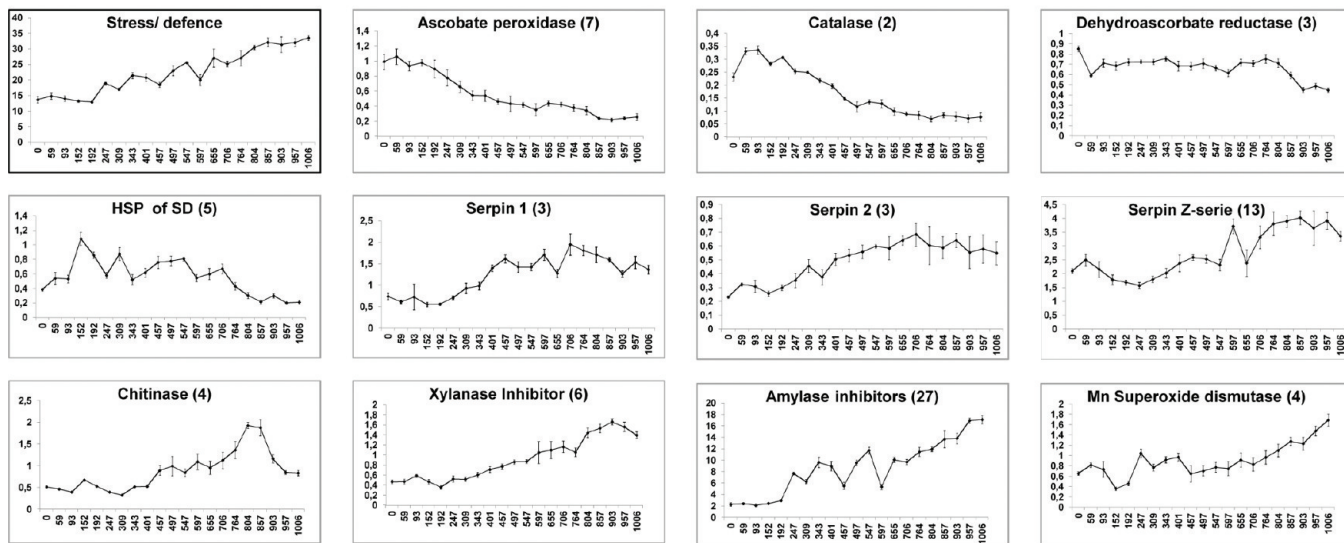


Figure 3. (a–h) Composite expression profiles of functional classes. The number of spots for the same category is indicated in parentheses. Each point is representative of the mean composite expression of normalized volume values of proteins (y-axis) at stages of development in °Cd (x-axis) and standard deviation $n = 6$.

Protein Functional Classification

Proteins were categorized in 17 different functional classes, using identified protein spots (487 out of 580). These spots were representative of all nine profiles (Table 1). This distribution differs not only between accumulation clusters but also within profiles of the same cluster (Figure 2).

The diversity of function was maximum in the early accumulation cluster (P1 and P2) with 14 different representative functions (Figure 2). In this cluster, dominating categories were carbohydrate metabolism (CM) with a 36% contribution in P1 and 24% in P2, followed by amino acid metabolism (AM) 14 and 15% respectively. Proteins related to

a**b**

kDa

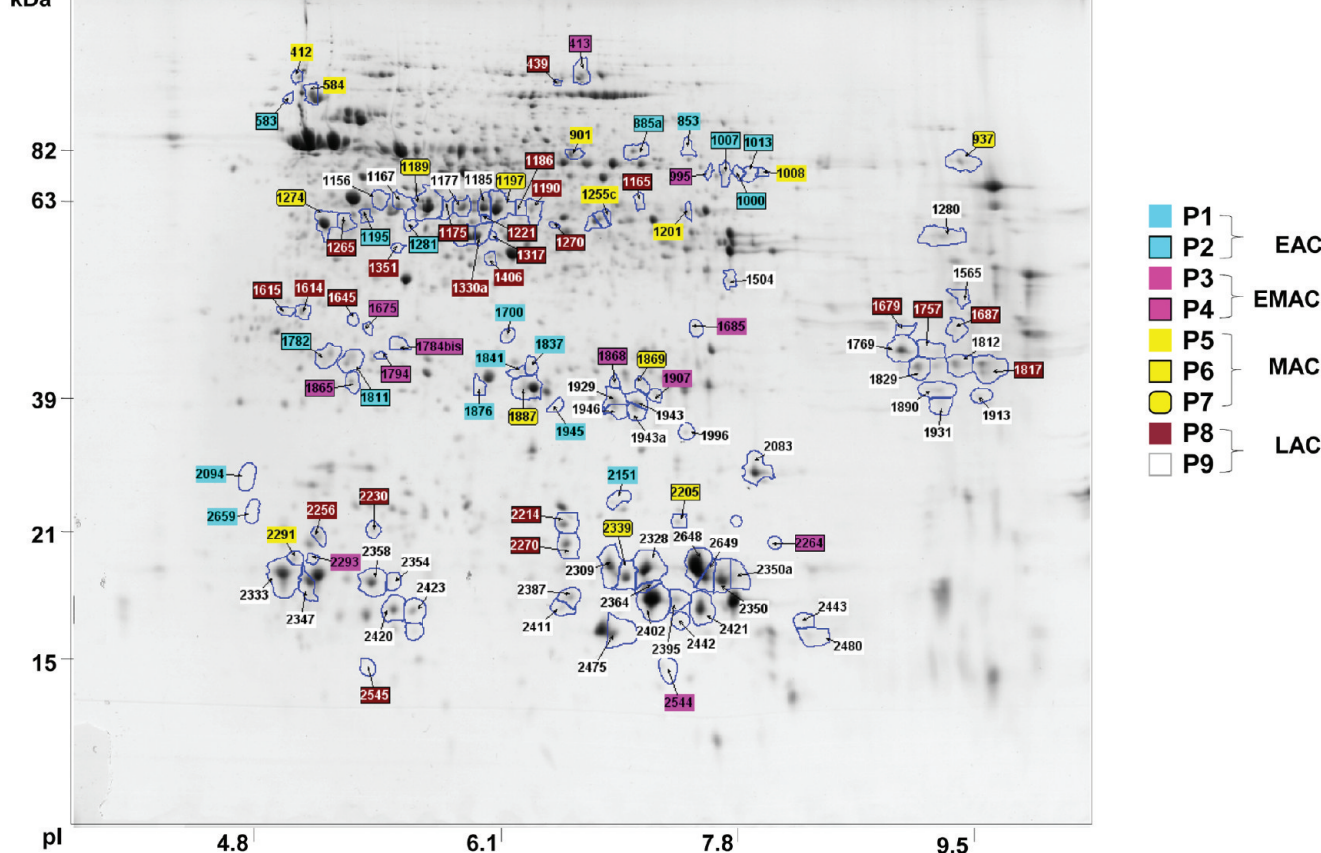


Figure 4. (a) Stress/defense and its subcategories representation, through their composite expression profiles. Composite expression of mean normalized volume values (y-axis) at 21 stages of development in °Cd (x-axis) with SD bars where $n = 6$. Total number of spots for each profile is indicated in parentheses. (b) Proteome map of stress/defense related proteins. Gel image is of 497 °Cd, and colored tags represent corresponding profiles of identified spot.

transcription/translation (Trs), ATP interconversion (AI), and protein transport (PT) were relatively more abundant in P2 than in P1.

P3 and P4, profiles of EMAC, were also dominated by CM (31 and 27% respectively). Significant changes in stress/defense (SD) (increase from 11 to 21%) AM (increase from 5 to 11%) and lipid metabolism (LM) (decrease from 6 to 3%) between

P3 and P4 were observed. In this cluster, protein folding (PF), protein synthesis (PS), and cell wall (CW) related proteins were specific to P4 while cell division (CD) and AI were only identified in P3.

Similar to EAC and EMAC, CM proteins were the dominant category also in MAC and increased from 26 to 48%, whereas a considerable decrease in Trs (19 to 5%) and ST (10 to 2%) was

observed. Notably, P6 displayed minimum (only 6) diversity of functions. The majority were CM (48%) and PS (32%), while AM, SD, PF and Trs were present at 5% each. In P7, SD (16%) and AM (9%) followed the largest category of CM proteins.

Remarkably, in LAC, dominance of CM was replaced by SD related proteins (50% in P8 and 58% in P9), while CM was reduced to 25 and 21% in P8 and P9 respectively. PS, AM and ST were significantly reduced while LM, Trs, CD, CK, AI and PT vanished completely from P9.

Composite Expression Profiles of Protein Functional Classes

This composite expression was calculated by summing normalized spot volumes of a given functional category, for all corresponding proteins¹⁴ (Figure 3).

Proteins involved in metabolism (LM, AM, CM, and NM) were abundant (Figure 3a,b,e,h) at early stages except folic acid metabolism (FM) (Figure 3g) where proteins accumulated toward grain maturity. CM as compared to AM, NM and LM showed nearly constant behavior throughout development with a slight gradual decrease in later developmental stages. Trs and ST attained a peak at 152 °Cd (Figure 3b,c) while PS and CD showed highest expression at 93 °Cd and 192 °Cd respectively (Figure 3b,a). CW related proteins were abundant at three early stages with a peak at 93 °Cd and afterward their level remained nearly constant (Figure 3a). Proteins related to AI category displayed a peak of expression at 152 °Cd, while those of PT were also abundant during early stages between 0 °Cd to 192 °Cd (Figure 3f,c).

Redox related proteins decreased with grain maturation (Figure 3d). At mid and mid late stages, proteins of CK, PF and SP were the dominating functional proteins (Figure 3c,d,f). Preponderance of SD and protein turn over (PTO) related proteins were shown at later stages of development (Figure 3e,g). SD protein subcategories are presented in Figure 4a. Although the SD category was dominant in later stages, composite expression profiles of its subcategories showed that all SD proteins were not dominant in LAC, but rather some were also abundantly present in EAC and MAC.

Prediction of Subcellular Protein Localization

Subcellular localization of identified proteins varied during development. In EAC proteins were scattered in eight different locations as compared to five in LAC. Cytoskeleton (cyk) proteins were found only in P1 and P2, nuclear (nucl) proteins from P1 to P7, while those of peroxisome (perox) in P1, P4 and P5. Proteins in cytosol (Cyto), endoplasmic reticulum (ER), extracellular region (extr), plastid (P), and mitochondria (M) were present throughout development. However, in Cyto they were abundant during early stages, in M and P during early and mid stages while those of ER and Extr were dominant in later stages (Figure S4, Supporting Information). Pathway and functional classifications were assigned for SD category proteins on the basis of ontology, and on metabolic features particularly established in plants (<http://metacyc.org>) (Figure S5, Supporting Information).^{29,30}

■ DISCUSSION

Wheat endosperm is a triploid tissue in which 80–85% of extractable proteins are gliadins and glutenins. Alg are less abundant proteins and consequently have been given less attention for grain quality improvement studies. Hand dissection of endosperm followed by protein extraction methods specific for alg proved to be efficient, as also revealed

by previous studies to determine their 2D patterns. In the present study, 21 stages were selected to develop a comprehensive proteome map of alg proteins during kernel development.

The total number of spots during development remained nearly constant with a slight decrease toward grain maturity. However, between developmental stages, relative abundance of individual spots was different, since image analysis detected 950 spots varying significantly between two or more stages. This protein spot variation provides evidence for coregulation, probable gene function that is activated or inactivated at specific phases and relationships between phases.

Nine accumulation profiles were distinguished by HCA and were grouped in four main clusters during alg temporal analysis. Proteins involved in carbohydrate metabolism, amino acid metabolism, and stress/defense were identified in all expression profiles. Transcription/translation was not identified in P8 and P9, while protein synthesis and protein folding mechanisms were not found in P3. Few functional categories appeared only in one or two accumulation profiles.

Early Accumulation Clusters (EAC and EMAC)

In early accumulation clusters (EAC and EMAC), EAC represented maximum functional diversity, with 14 different functions in both P1 and P2 (Figure 2). The highest number of proteins was identified in P1 among nine profiles, with a majority of proteins involved in CM. In early stages of development, wheat caryopsis changes dramatically in size and shape, and study of caryopsis structure revealed that, in endosperm at 3 DAP (≈ 60 °Cd), a single layer of free nuclei is present only around the central vacuole.³¹ At 6 DAP (≈ 110 °Cd), in parallel to caryopsis development, these nuclei are present in the whole central region that was occupied by the central vacuole because of cellularization of peripheral endosperm. All major cell types are differentiated around 13 DAP (≈ 250 °Cd).³² CD and CK related proteins are thought to play significant roles in these developmental processes. Microtubules (CD) and actin filaments (CK) are not only important for cell growth and division but they also target organelles and vesicles.³³ To participate in above-mentioned tasks, CD and CK were maximum at 192 °Cd, the period before the start of grain filling (Figure 3a,c). Enzymes for LM were also abundant in EAC and EMAC. These enzymes, together with CD and CK related proteins, take part in cell division, cell expansion, differentiation, sequential and continuous processes involving cessation of sucrose uptake, and accumulation of storage products.

Sucrose and nitrogen are taken up by seeds in the form of amino acids from the apoplast,³⁴ and generally biosynthesis of seed storage protein is dependent on enzymes of nitrogen metabolism.^{35,36} Enzymes for synthesis of amino acids such as phenylalanine, tyrosine, serine, homocysteine, cysteine, proline, glycine, aspartate, glutamic acid, methionine, threonine were identified. In addition, two other amino acids, acetohydroxyacid synthase (involved in biosynthesis of leucine, isoleucine and valine)³⁷ and ketolacid reductoisomerase responsible for isoleucine and valine biosynthesis were also found. These enzymes were abundant in EAC and EMAC (prestorage phase) and attenuated with grain maturity.

Mid Accumulation Cluster (MAC)

In this cluster we found some proteins of prestorage and mainly of storage phase. This cluster was dominated by CM, SD, Trs, and AM. CM continued to be the principal metabolism, and in

P6 and P7 its participation was highest (48%) among all profiles (Figure 2). A study by Lunn et al. supported the proposal that the changes induced in the rate of starch synthesis by sucrose are mediated by trehalose-6-phosphate (Tre 6P), as they found it as a signaling metabolite of sugar status in plants.³⁸ In wheat, Tre 6P expression is tissue and developmental stage dependent, at 7 DAP (≈ 130 °Cd), its level was nearly same in both maternal and filial tissues but at grain filling stage 17 DAP (≈ 320 °Cd), accumulation was mostly restricted to endosperm.³⁹ Enzymes involved in sucrose and starch metabolism were found abundantly in this cluster, complementing the above results where starch synthesis was higher at 17 DAP (≈ 320 °Cd).

Starch biosynthesis and accumulation is the major process of grain filling and four principal enzymes sucrose synthase, ADP glucose pyrophosphate, starch branching enzyme (SBE) and starch synthase are involved.⁴⁰ Accordingly, sucrose synthase, SBE and ADP glucose pyrophosphate relative abundances were found maximum between 152 and 706 °Cd with peak at 597 °Cd. A starch synthesis regulatory enzyme, alpha 1,4-glucan phosphorylase,⁴¹ accumulated also between 152 and 706 °Cd. These four curves indicated that, for accumulation of enzymes involved in the biosynthesis of starch, the critical period lies between 152 and 706 °Cd. (Figure S6a, Supporting Information)

Programmed cell death (PCD) in cereal endosperm moves in parallel to grain filling. Studies on developing wheat endosperm revealed that PCD was first detected at 16 DAP (≈ 300 °Cd), and finished with starch and protein accumulation.^{42,43} In our study, the four identified SP peaked at 706 °Cd, (Figure 3f) the period of endosperm development completion.⁴³ They had an expression curve similar to those of MAC, i.e., no or very low expression in the early and late stages and high expression in the middle stages of development. At the start of grain filling a high sugar level may be involved indirectly for ethylene production, which is an important key for PCD onset in developing endosperm.⁴⁴ At 30 DAP (≈ 580 °Cd), PCD penetrates in whole endosperm, and its products (mainly proteases in plants) increased as revealed by the peak of proteasomes, which increased after 597 °Cd until 1006 °Cd (Figure S6b, Supporting Information). A reduction in the accumulation of translation initiation factors decreased protein synthesis which is probably also a result of PCD (Figure 3b). Cell death is also strongly influenced by oxidative stress.

The absence of stomata, as well as the presence of several outer seed layers, acts as diffusion barriers within tissues and results in hypoxia that leads to low energy production. The redox mechanism was highly active at early stages of development because of the permeability of the young pericarp and photosynthetic mechanism of peripheral grain layers that are still green.⁴⁵ In developing seeds, a struggle for energy and oxygen was noticed from the reserve accumulation stage to desiccation period,⁴⁵ and there we observed a decrease of the redox curve (Figure 3d). During wheat kernel development, ambient oxygen was found to be hypoxic.⁴⁶ With less oxygen availability, primary metabolism activity slows down, or switches to metabolic pathways with less ATP consumption.^{47,48} Accordingly, AI and CW in addition to nearly all metabolic processes (CM, AM, LM, NM), except FM, decreased (Figure 3). These metabolic changes were found to be due to membrane alterations and less seed respiration caused by an adaptive response to avoid or to postpone plant

tissues from suffering anoxia and its concomitant negative effects.⁴⁹

Late Accumulation Cluster (LAC)

P8 and P9 represent the proteins of LAC that were found to be abundant in grain maturity stages. Composite protein expression curves revealed that these stages were dominated by the proteins involved in SD, PTO and FM. An increase in PTO curve was mainly due to proteasome proteins discussed above in PCD. In P8 one gamma-gliadin was identified. Normally gamma-gliadin possesses eight cysteins. Sequence inquiry revealed strong similarity with gliadin/avenin-like seed proteins (commonly found in alg preparations) and an even number (six) of cysteine giving three intramolecular disulfide bonds. This made gamma-gliadin partially soluble and unpolymerized with other storage proteins; hence it was extracted with soluble proteins of alg.

SD Enzymes

In SD, proteins related to both biotic and abiotic stresses were found abundantly in LAC, with continuous increase from 247 °Cd up to 1006 °Cd. These proteins at EAC and EMAC were present from acidic to central (neutral) part of the gels, while in the basic zone, there were only the proteins of later stages particularly of P8 and P9 (Figure 4b).

Subcellular localization of SD proteins revealed that the majority of these proteins were in cytosol (35%) and extracellular region (29%); they were comparatively less abundant in P (20%) and ER (11%) while only few were observed in perox (3%), M (2%) and nucl (1%). In early developmental stages proteins were abundant mostly in cytosol, with only little number in other localizations. In parallel with grain development they appeared abundantly in several localizations, as in P9 they were predicted significantly in four different localizations, i.e., cyto, P, Extr, and ER. (Figure 5).

Metabolic pathways of SD category enzymes are presented in (Figure S5, Supporting Information). This provided a rapid overview of SD enzymes and also specifies their position in the developmental scale. ROS related enzymes were found to be abundant during EAC and EMAC, as can be seen from composite expression curves of catalase, ascorbate peroxidase,

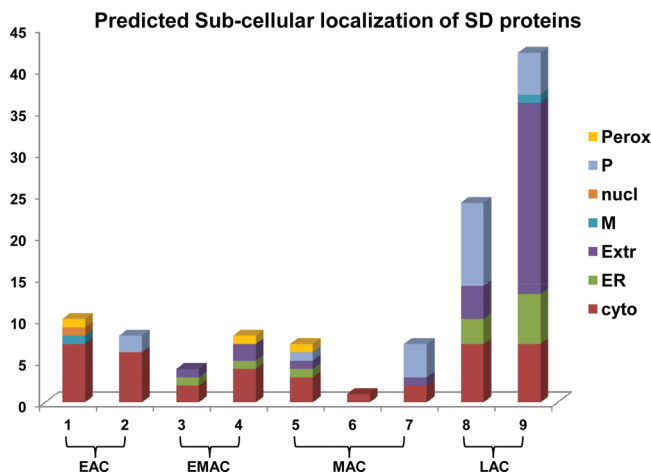


Figure 5. Predicted stress/defense protein distribution in different subcellular localizations. X-axis represents profiles (P1–P9), while y-axis represents the number of identified proteins in corresponding profiles. Cyto, cytosol; ER, endoplasmic reticulum; Extr, extra-cellular region; M, mitochondria; nucl, nuclear; P, plastid; Perox, peroxisome.

dehydro ascorbate reductase (Figure 4a). These enzymes were abundant in cytosol in early stages for processes such as detoxification and dehydrogenation. In these stages enzymes present in Perox were for catabolism of long chain fatty acids, and LM abundance thus decreased toward maturity (Figure 3a). Abiotic stress related proteins such as salt tolerant protein and Wali 7 (Al stress related) were observed also in early accumulation clusters, probably for assistance of healthy seed development.

Five heat shock proteins involved in SD were observed in P2, P4, P5 and P8. High molecular weight HSPs such as 101 were found in cyto; these are chaperons in nature and are involved in refolding of proteins that are denatured during EMAC (spot 413) and LAC (spot 439). In MAC, HSP90 were located in cyto (584) and ER (412). They were active in parallel with PF (Figure 3d) as they help in stabilizing proteins prior to complete folding. Briefly, HSP network was found functional throughout development during three different compartments.

Inhibitors of xylanase, alpha-amylase and serine proteinase along with chitinases were found to be abundant in later stages (Figure 4a), and their possible role in different pathways is indicated (Figure S5, Supporting Information). In addition to their role in starch mobilization, alpha amylase inhibitors are involved in many other functions; for example, they serve as storage proteins, provide essential amino acids for human nutrition, have protective role and are also involved in wheat allergies.⁵⁰

LAC proteins were predicted mainly in four different localizations. Serpins, which are a complex-natured protein family, were found in P, abundantly in MAC (P5 and P7) and in both profiles of LAC. It was found that wheat serpins may have a protective role for prolamins,⁵¹ which are present around the amyloplasts. They probably also protect starch, which shared the same subcellular localization as serpins. Extracellular region proteins, which are either synthesized directly in this region or came through secretory pathway,⁵² were principally inhibitors of alpha amylase and xylanase. These proteins while residing in plasma membrane help in protecting the cellular contents of dehydrated grain. Well-established grain protective mechanisms were found to be active during grain development, particularly in extracellular region at later stages.

Study of grain development with monitoring at every 50 °Cd provided not only an insight into the major events but also a more precise understanding of the occurrence of these events (in terms of composite expression profiles for a given functional category). In a previous study while comparing two stages, 10 DAP (\approx 200 °Cd) and 36 (\approx 700 °Cd), PT and AI proteins were found to be abundant at 700 °Cd.¹⁹ In contrast we found that PT and AI peaked at 192 and 152 °Cd respectively, and then decreased with grain maturity (Figure 3c,f). This difference could result from the lower number of proteins identified (4 vs 8 for PT and 2 vs 13 for AI) in earlier study, which also revealed that SP expression peaked at 700 °Cd. The findings in the present experiment not only validated SP results, but also it was noticed that, after 700 °Cd, expression decreased significantly for SP (Figure 3f). This decrease of SP may be due to their remobilization for accumulation of other proteins in later stages. Seven PTO identified by Vensel et al. were found abundant at 200 °Cd, whereas no significant differences were found between 200 and 700 °Cd for 21 PTO identified in the present study. In addition, after 700 °Cd they increased toward grain maturity (Figure 3g).

Despite these differences, this study helped us to reveal the expression behavior throughout development for proteins, whose expression was found common between these two studies at both developmental stages. As for proteins that were observed abundantly at 200 °Cd, we additionally found that CM and AM decrease linearly, CD, ST and LM were highly abundant in early grain development stages and then decreased significantly, while CK proteins appeared uniformly between 152 and 597 °Cd. Similarly, the SD category, which increased towards grain maturity in both studies, showed a linear increase from 247 °Cd until maturity.

This study with 21 stages unraveled the alg protein expression during whole grain development and provided valuable information that complemented the events known up to present. In addition to four main phases of development, three subphases in phase three and two in phase 4 were evident. In this study we constructed an alg proteome reference map with nine submaps on the basis of corresponding expression profiles not so far described, as previous studies were on limited scale of development in terms of number and interval.^{18–20} Additional areas need to be explored, such as comparison between expression profiles of metabolic processes by mining of different wheat tissues or by performing the different “omics” analysis for development of comprehensive understanding of wheat grain development. This reference study could be used for investigation of biotic and abiotic stress responses. Study of alg and gluten proteins during development would help to explore the influence of soluble proteins on accumulation of storage proteins.

■ ASSOCIATED CONTENT

S Supporting Information

Figures S1–S6 and Table S1. This material is available free of charge via the Internet at <http://pubs.acs.org>.

■ AUTHOR INFORMATION

Corresponding Author

*E-mail: branlard@clermont.inra.fr. Tel.: +33 (0)473624316. Fax: +33 (0)473624453.

Notes

The authors declare no competing financial interest.

■ ACKNOWLEDGMENTS

We acknowledge gratefully Didier Viala for MS analysis, Said Mouzeyar, Emmanuelle Bancel, and Felicity Vear for critical reading, and Higher Education Commission, Pakistan for financial support.

■ ABBREVIATIONS:

°Cd, degree days after pollination; alg, albumins globulins; EAC, early accumulation cluster; EMAC, early mid accumulation cluster; MAC, mid accumulation cluster; LAC, late accumulation cluster; HCA, hierarchical cluster analysis; PCA, principal component analysis

■ REFERENCES

- (1) Bietz, J. A.; Wall, J. S. Wheat gluten subunits: Molecular weight determined by sodium deodecyl sulfate-polyacrylamide gel electrophoresis. *Cereal Chem.* **1972**, *49* (4), 416–430.
- (2) Brown, J. W. S.; Flavell, R. B. Fractionation of wheat gliadin and glutenin subunits by two-dimensional electrophoresis and the role of

- group-6 and group-2 chromosomes in gliadin synthesis. *Theor. Appl. Genet.* **1981**, *59* (6), 349–359.
- (3) Islam, N.; Woo, S. H.; Tsujimoto, H.; Kawasaki, H.; Hirano, H. Proteome approaches to characterize seed storage proteins related to ditelocentric chromosomes in common wheat (*Triticum aestivum* L.). *Proteomics* **2002**, *2* (9), 1146–1155.
- (4) Branlard, G.; Dumur, J.; Bancel, E.; Merlin, M.; Dardevet, M. Proteomic analysis of wheat storage proteins: A promising approach to understand the genetic and molecular bases of gluten components, *The Gluten proteins*, Royal Society of Chemistry: Cambridge, U.K., 2004, Issue 295, pp 30–33.
- (5) Tosi, P.; Gritsch, C. S.; He, J. B.; Shewry, P. R. Distribution of gluten proteins in bread wheat (*Triticum aestivum*) grain. *Ann. Bot.* **2011**, *108* (1), 23–35.
- (6) Pomeranz, Y. *Wheat: Chemistry and Technology*, AAC Monograph Series; American Association of Cereal Chemists: St Paul, MN, USA, 1988; Vol. I.
- (7) Hill, K.; Horvath-Szánics, E.; Hajos, G.; Kiss, E. Surface and interfacial properties of water-soluble wheat proteins. *Colloids Surf, A* **2008**, *319* (1–3), 180–187.
- (8) Singh, J.; Skerritt, J. H. Chromosomal control of albumins and globulins in wheat grain assessed using different fractionation procedures. *J. Cereal Sci.* **2001**, *33* (2), 163–181.
- (9) Koch, K. Sucrose metabolism: regulatory mechanisms and pivotal roles in sugar sensing and plant development. *Curr. Opin. Plant Biol.* **2004**, *7* (3), 235–246.
- (10) Wobus, U.; Weber, H. Sugars as signal molecules in plant seed development. *Biol. Chem.* **1999**, *380* (7–8), 937–944.
- (11) Borisjuk, L.; Rolletschek, H.; Radchuk, R.; Weschke, W.; Wobus, U.; Weber, H. Seed development and differentiation: A role for metabolic regulation. *Plant Biol.* **2004**, *6* (4), 375–386.
- (12) Tasleem-Tahir, A.; Nadaud, I.; Girousse, C.; Martre, P.; Marion, D.; Branlard, G. Proteomic analysis of peripheral layers during wheat (*Triticum aestivum* L.) grain development. *Proteomics* **2011**, *11* (3), 371–379.
- (13) Finnie, C.; Melchior, S.; Roepstorff, P.; Svensson, B. Proteome analysis of grain filling and seed maturation in barley. *Plant Physiol.* **2002**, *129* (3), 1308–1319.
- (14) Mechlin, V.; Thevenot, C.; Le Guilloux, M.; Prioul, J. L.; Damerval, C. Developmental analysis of maize endosperm proteome suggests a pivotal role for pyruvate orthophosphate dikinase. *Plant Physiol.* **2007**, *143* (3), 1203–1219.
- (15) Gallardo, K.; Le Signor, C.; Vandekerckhove, J.; Thompson, R. D.; Burstin, J. Proteomics of *Medicago truncatula* seed development establishes the time frame of diverse metabolic processes related to reserve accumulation. *Plant Physiol.* **2003**, *133* (2), 664–682.
- (16) Houston, N. L.; Hajduch, M.; Thelen, J. J. Quantitative proteomics of seed filling in castor: comparison with soybean and rapeseed reveals differences between photosynthetic and non-photosynthetic seed metabolism. *Plant Physiol.* **2009**, *151* (2), 857–868.
- (17) Singh, J.; Blundell, M.; Tanner, G.; Skerritt, J. H. Albumin and globulin proteins of wheat flour: Immunological and N-terminal sequence characterisation. *J. Cereal Sci.* **2001**, *34* (1), 85–103.
- (18) Wong, J. H.; Cal, N.; Balmer, Y.; Tanaka, C. K.; Vensel, W. H.; Hurkman, W. J.; Buchanan, B. B. Thioredoxin targets of developing wheat seeds identified by complementary proteomic approaches. *Phytochemistry* **2004**, *65* (11), 1629–1640.
- (19) Vensel, W. H.; Tanaka, C. K.; Cai, N.; Wong, J. H.; Buchanan, B. B.; Hurkman, W. J. Developmental changes in the metabolic protein profiles of wheat endosperm. *Proteomics* **2005**, *5* (6), 1594–1611.
- (20) Gao, L. Y.; Wang, A. L.; Li, X. H.; Dong, K.; Wang, K.; Appels, R.; Ma, W. J.; Yan, Y. M. Wheat quality related differential expressions of albumins and globulins revealed by two-dimensional difference gel electrophoresis (2-D DIGE). *J. Proteomics* **2009**, *73* (2), 279–296.
- (21) Debiton, C.; Merlin, M.; Chambon, C.; Bancel, E.; Decourteix, M.; Planchot, V.; Branlard, G. Analyses of albumins, globulins and amphiphilic proteins by proteomic approach give new insights on waxy wheat starch metabolism. *J. Cereal Sci.* **2011**, *53* (2), 160–169.
- (22) Bradford, M. M. Rapid and sensitive method for quantitation of microgram quantities of protein utilizing principle of protein-dye binding. *Anal. Biochem.* **1976**, *72* (1–2), 248–254.
- (23) Altschul, S. F.; Madden, T. L.; Schaffer, A. A.; Zhang, J. H.; Zhang, Z.; Miller, W.; Lipman, D. J. Gapped BLAST and PSI-BLAST: a new generation of protein database search programs. *Nucleic Acids Res.* **1997**, *25* (17), 3389–3402.
- (24) Horton, P.; Park, K. J.; Obayashi, T.; Fujita, N.; Harada, H.; Adams-Collier, C. J.; Nakai, K. WoLF PSORT: protein localization predictor. *Nucleic Acids Res.* **2007**, *35*, W585–W587.
- (25) Small, I.; Peeters, N.; Legeai, F.; Lurin, C. Predotar: A tool for rapidly screening proteomes for N-terminal targeting sequences. *Proteomics* **2004**, *4* (6), 1581–1590.
- (26) Emanuelsson, O.; Nielsen, H.; Brunak, S.; von Heijne, G. Predicting subcellular localization of proteins based on their N-terminal amino acid sequence. *J. Mol. Biol.* **2000**, *300* (4), 1005–1016.
- (27) Briesemeister, S.; Rahnenfuhrer, J.; Kohlbacher, O. YLoc-an interpretable web server for predicting subcellular localization. *Nucleic Acids Res.* **2010**, *38*, W497–W502.
- (28) Chi, S. M.; Nam, D. WegoLoc: accurate prediction of protein subcellular localization using weighted Gene Ontology terms. *Bioinformatics* **2012**, DOI: 10.1093/bioinformatics/bts062.
- (29) Buchanan, B. B.; Gruissem, W.; Jones, R. L. *Biochemistry and Molecular Biology of Plants*; American Society of Plant Physiology: Rockville, MD, 2000.
- (30) Catusse, J.; Strub, J. M.; Job, C.; Van Dorsselaer, A.; Job, D. Proteome-wide characterization of sugarbeet seed vigor and its tissue specific expression. *Proc. Natl. Acad. Sci. U. S. A.* **2008**, *105* (29), 10262–10267.
- (31) Sabelli, P. A.; Larkins, B. A. The Development of Endosperm in Grasses. *Plant Physiol.* **2009**, *149* (1), 14–26.
- (32) Drea, S.; Leader, D. J.; Arnold, B. C.; Shaw, P.; Dolan, L.; Doonan, J. H. Systematic spatial analysis of gene expression during wheat caryopsis development. *Plant Cell* **2005**, *17* (8), 2172–2185.
- (33) Mayer, U.; Jürgens, G. Microtubule cytoskeleton: a track record. *Curr. Opin. Plant Biol.* **2002**, *5* (6), 494–501.
- (34) Weber, H. Molecular physiology of legume seed development. *Annu. Rev. Plant Biol.* **2005**, *56*, 253–279.
- (35) Balconi, C.; Rizzi, E.; Manzocchi, L.; Soave, C.; Motto, M. Analysis of in vivo and in vitro grown endosperms of high and low protein strains of maize. *Plant Sci.* **1991**, *73* (1), 1–9.
- (36) Hernandez-Sebastia, C.; Marsolais, F.; Saravitz, C.; Israel, D.; Dewey, R. E.; Huber, S. C. Free amino acid profiles suggest a possible role for asparagine in the control of storage-product accumulation in developing seeds of low- and high-protein soybean lines. *J. Exp. Bot.* **2005**, *56* (417), 1951–1963.
- (37) Duggleby, R. G.; Pang, S. S. Acetohydroxyacid synthase. *J. Biochem. Mol. Biol.* **2000**, *33* (1), 1–36.
- (38) Lunn, J. E.; Feil, R.; Hendriks, J. H. M.; Gibon, Y.; Morcuende, R.; Osuna, D.; Scheible, W. R.; Carillo, P.; Hajirezaei, M. R.; Stitt, M. Sugar-induced increases in trehalose 6-phosphate are correlated with redox activation of ADPglucose pyrophosphorylase and higher rates of starch synthesis in *Arabidopsis thaliana*. *Biochem. J.* **2006**, *397*, 139–148.
- (39) Martinez-Barajas, E.; Delatte, T.; Schluepmann, H.; de Jong, G. J.; Somsen, G. W.; Nunes, C.; Primavesi, L. F.; Coello, P.; Mitchell, R. A. C.; Paul, M. J. Wheat grain development is characterized by remarkable trehalose 6-phosphate accumulation pregrain filling: Tissue distribution and relationship to SNF1-related protein kinase1 activity. *Plant Physiol.* **2011**, *156* (1), 373–381.
- (40) Yang, J. C.; Zhang, J. H.; Wang, Z. Q.; Xu, G. W.; Zhu, Q. S. Activities of key enzymes in sucrose-to-starch conversion in wheat grains subjected to water deficit during grain filling. *Plant Physiol.* **2004**, *135* (3), 1621–1629.
- (41) Tickle, P.; Burrell, M. M.; Coates, S. A.; Emes, M. J.; Tetlow, I. J.; Bowsher, C. G. Characterization of plastidial starch phosphorylase in *Triticum aestivum* L. endosperm. *J. Plant Physiol.* **2009**, *166* (14), 1465–1478.

- (42) Young, T. E.; Gallie, D. R. Analysis of programmed cell death in wheat endosperm reveals differences in endosperm development between cereals. *Plant Mol. Biol.* **1999**, *39* (5), 915–926.
- (43) Rui, L.; Sheng-Yin, L.; Zhen-Xiu, X. Programmed cell death in wheat during starchy endosperm development. *J. Plant Physiol. Mol. Biol.* **2004**, *30* (2), 183–188.
- (44) Young, T. E.; Gallie, D. R. Programmed cell death during endosperm development. *Plant Mol. Biol.* **2000**, *44* (3), 283–301.
- (45) Angelovici, R.; Galili, G.; Fernie, A. R.; Fait, A. Seed desiccation: a bridge between maturation and germination. *Trends Plant Sci.* **2010**, *15* (4), 211–218.
- (46) van Dongen, J. T.; Roeb, G. W.; Dautzenberg, M.; Froehlich, A.; Vigeolas, H.; Minchin, P. E. H.; Geigenberger, P. Phloem import and storage metabolism are highly coordinated by the low oxygen concentrations within developing wheat seeds. *Plant Physiol.* **2004**, *135* (3), 1809–1821.
- (47) Huang, S. B.; Colmer, T. D.; Millar, A. H. Does anoxia tolerance involve altering the energy currency towards PPi? *Trends Plant Sci.* **2008**, *13* (5), 221–227.
- (48) Vigeolas, H.; van Dongen, J. T.; Waldeck, P.; Huhn, D.; Geigenberger, P. Lipid storage metabolism is limited by the prevailing low oxygen concentrations oilseed rape. *Plant Physiol.* **2003**, *133* (4), 2048–2060.
- (49) Geigenberger, P. Response of plant metabolism to too little oxygen. *Curr. Opin. Plant Biol.* **2003**, *6* (3), 247–256.
- (50) Altenbach, S. B.; Vensel, W. H.; Dupont, F. M. The spectrum of low molecular weight alpha-amylase/protease inhibitor genes expressed in the US bread wheat cultivar Butte 86. *BMC Res. Notes* **2011**, *4*, 242.
- (51) Ostergaard, H.; Rasmussen, S. K.; Roberts, T. H.; Hejgaard, J. Inhibitory serpins from wheat grain with reactive centers resembling glutamine-rich repeats of prolamin storage proteins — Cloning and characterization of five major molecular forms. *J. Biol. Chem.* **2000**, *275* (43), 33272–33279.
- (52) Rose, J. K. C.; Lee, S. J. Straying off the Highway: Trafficking of secreted plant proteins and complexity in the plant cell wall proteome. *Plant Physiol.* **2010**, *153* (2), 433–436.